ELSEVIER

Materials Chemistry and Physics 67 (2001) 92–100

MATERIALS CHEMISTRY AND PHYSICS

www.elsevier.com/locate/matchemphys

The liquid phase sintering of molybdenum with Ni and Cu additions

K.S. Hwang*, H.S. Huang

Institute of Materials Science and Engineering, National Taiwan University, 1, Roosevelt Road, Sec. 4, Taipei 106, Taiwan, ROC

Abstract

To increase the sintered density of Mo compacts, liquid phase sintering was employed by adding sintering aids, Ni and Cu. With 1.5 wt.% Ni sintered at 1370°C, the sintered density of Mo increased from 86.0 to 97.5%. When one-third of the Ni was replaced by Cu, the density was improved from 82.1 to 99.1% when sintered at 1300°C. Although copper has little solubility in molybdenum, and vice versa, it aids nickel in enhancing the sintering of molybdenum compact during heating in the solid state and during the liquid phase sintering. The dilatometer run indicated that the liquid formation temperature was lowered by 90°C. Better wetting on molybdenum particles was also observed. However, the Mo–Ni–Cu compact was still brittle due to the presence of brittle Mo–Ni compounds at the grain boundaries.

Keywords: Liquid phase sintering; Molybdenum; Mo–Ni–Cu

1. Introduction

Molybdenum is known as a refractory metal, and its sintering temperature is usually greater than 1700°C. At such a high temperature, specialized vacuum or hydrogen furnaces with graphite or tungsten heaters are required. The large amount of energy consumed is also a cost concern. To facilitate the sintering of molybdenum, two common techniques are employed; liquid phase sintering and solid state activated sintering [1–3].

Activated sintering has been studied since the early 1960s [4,5]. With a small amount of activator, such as Ni, Pd, or Pt, the sintered density can be significantly enhanced. It is generally believed that, during activated sintering, one role of the activators is to form a thin layer on the Mo surface, which provides a short-circuit diffusion path for Mo atoms. The other role is to increase the grain boundary diffusion coefficient of molybdenum [3,4,6].

Another technique, liquid phase sintering, has also been used to improve the sintering of Mo and W. The liquid phase plays a role similar to the activators in activated solid state sintering. Unfortunately, these two techniques are not widely used in the molybdenum and tungsten industry due to the poor ductility of sintered compacts. The cause of such brittleness is still not clearly understood. However, it is generally accepted that grain coarsening [7] and the segregation of Ni-rich layers [2,8] are the two most likely causes. In improving the ductility of the Mo–Ni compacts, detailed knowledge of these two factors is important.

Although the addition of a single transition metal element does not help the W and Mo industries due to the negligible ductility, the ternary system with the liquid phase sintering technique is widely used. The typical examples are the W–Ni–Fe and W–Ni–Cu tungsten-based alloys, which could have more than 10% elongation [9,10]. Several recent studies have revealed that when binary activators, such as Ni–Fe, Ni–Cr [11], Ni–Co [12], and Ni–Al [13] are employed, the sintering of molybdenum becomes more enhanced than is possible by adding single elements. However, the use of the Ni–Cu mixture, which is frequently used on tungsten-based heavy metals, has not been investigated on molybdenum.

In this study, enhanced sintering of molybdenum powder compacts was investigated by using the liquid phase sintering technique. Since most shrinkage occurred during heating in the solid state, the effect of activated sintering was also investigated.

2. Experimental procedure

Three powders, Mo, Ni, and Cu were used in this study. The characteristics and the morphology of the three powders are given in Table 1 and Fig. 1, respectively. To prepare the compact, molybdenum powders were mixed with different amounts of Ni or Ni and Cu powders in a V-shaped mixer for 1 h. The mixed powders were compacted to rectangular bars of 40 mm × 15 mm × 4.3 mm using a pressure of 450 MPa. The green density was 67.5 ± 1%. For Mo–Ni compacts, the sintering was carried out at 1300°C (activated

* Corresponding author.

0254-0584/01/$ – see front matter
PII: S0254-0584(00)00425-9

Table 1
Characteristics of the Mo, Ni, and Cu powders used in this study

Powder	Mo	Ni	Cu
Grade	OMP901	Ni-123	Cu-635
Supplier	CSM	INCO	ACuPowder
Density, $g\,cm^{-3}$ (pycnometer)	10.18	8.89	8.71
Chemistry			
C (%)	0.0019	0.0808	0.2671
S (%)	0.0013	0.0001	0.0023
O (%)	0.9268	0.1955	0.4129
N (%)	0.0088	0.0015	0.0092

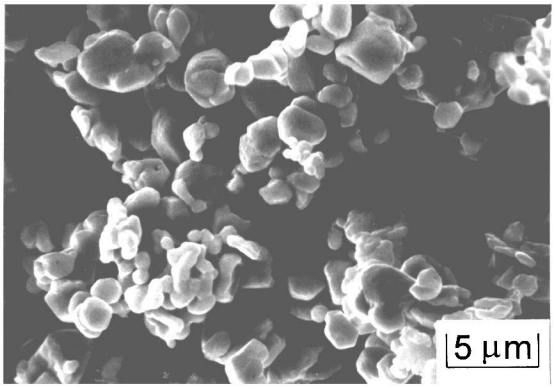

(a)

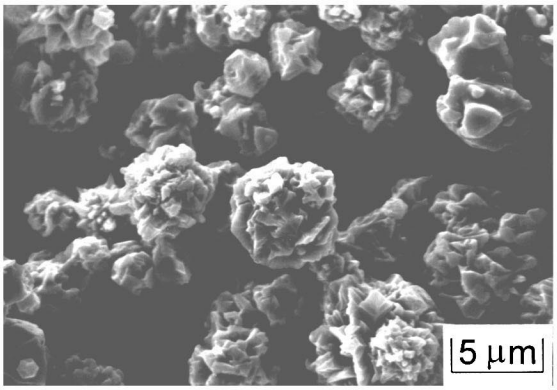

(b)

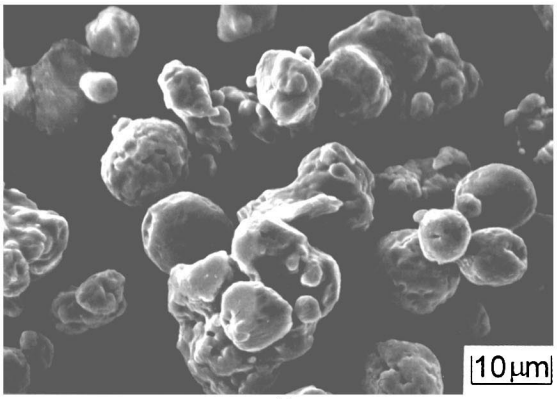

(c)

Fig. 1. Morphologies of the powders used in this study: (a) Mo, (b) Ni, and (c) Cu.

sintering) and 1370°C (liquid phase sintering), respectively, for 1 h in hydrogen. For Mo–Ni–Cu systems, compacts were sintered at 1300°C (liquid phase sintering), also for 1 h in hydrogen. To understand the sintering behavior, compacts were also heated at a rate of $10^{\circ}C\,min^{-1}$ in a dilatometer under hydrogen.

The sintered densities were measured by the Archimedes method. Bending strength was determined by the 4-point bending test at a crosshead speed of $2.5\,mm\,min^{-1}$. The hardness was measured with a Vickers microhardness tester (MVK-E2, Akashi, Tokyo, Japan) using a 50 g load. Both optical and scanning electron microscopes (SEM) were used to analyze the microstructure. The etchant used on polished specimens was the Murakami agent. For chemical analysis, an electron probe microanalyzer (EPMA, 8600SX, JEOL, Tokyo, Japan) was used to measure the amount of the elements at different phases. For the chemical composition at grain boundaries, specimens were fractured inside a Scanning Auger Microscope (SAM660, Perkin Elmer, MN, USA) under high vacuum (4×10^{-10} torr) so that the fractured surfaces were not contaminated. The depth profile of Ni and Cu on the Mo surfaces was taken using Ar ion sputtering. The sputtering rate was $1\,nm\,min^{-1}$ with reference to a Ta_2O_5 standard.

3. Results

Fig. 2 shows the density of Mo with 1.5 wt.% additives composed of different ratios of Ni and Cu after being sintered at 1300°C for 1 h. The Mo–1.5 wt.% Ni compact reached 95.5% density. As some Ni was replaced by Cu, the sintered density increased, reaching the maximum of 99.1% at 16.7 wt.% Cu (5Ni/1Cu) and 33.3 wt.% Cu (2Ni/1Cu), and then decreased to 81.8% at Mo–1.5 wt.% Cu, which is close to the 82.1% density of the pure Mo compact without Ni or Cu additions. This shows that pure Cu did not enhance sintering of Mo. However, when combined with Ni, such as Mo–1.0 wt.% Ni–0.5 wt.% Cu and Mo–1.25 wt.% Ni–0.25 wt.% Cu, its enhancement effect is better than the

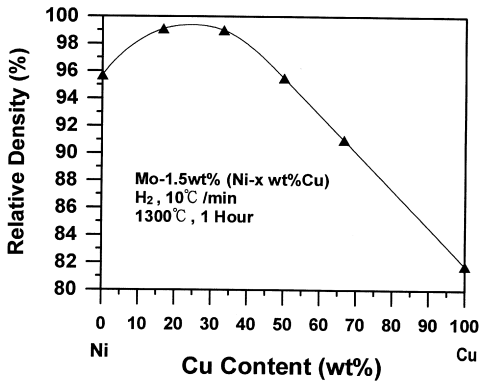

Fig. 2. The sintered density of Mo compacts with 1.5 wt.% additives with different ratios of Ni and Cu.

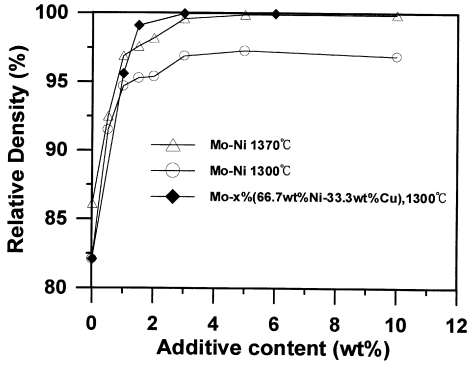

Fig. 3. The effects of Ni and Ni–Cu (at 2:1 ratio) content on the density of Mo compacts which are sintered at 1300 and 1370°C for 1 h.

Mo–1.5 wt.% Ni. For further detailed studies on the properties and sintering behavior of Mo–Ni–Cu compacts, a fixed Ni/Cu ratio of 2 to 1 was used.

The effect of the total amount of additives was also examined. Fig. 3 shows that for activated sintering of Mo–Ni at 1300°C, a small amount of Ni drastically improved the sintered density. As the amount of Ni increased to 5 wt.%, the density reached the plateau of 97%. For liquid phase sintering of Mo–Ni at 1370°C, the density curve has the same trend as that of the 1300°C, but the final density increased to 99.5% at 5 wt.% Ni addition. With the liquid phase sintering of Mo–Ni–Cu (at a fixed Ni/Cu ratio of 2) at 1300°C, the sintered density was further improved compared to the Mo–Ni system. Since 1.5 wt.% additive is enough to show enhancement, the following experiments were performed by using mainly the Mo–1.0 wt.% Ni–0.5 wt.% Cu and Mo–1.5 wt.% Ni alloys.

Fig. 4 compares the density of Mo–Ni and Mo–Ni–Cu compacts sintered for 1 h at different temperatures. The density of the Mo–Ni compacts increased as the sintering temperature increased from 1200 to 1400°C. With Cu additions, the sintered density reached the maximum at 1300°C. Further increase in the sintering temperature did not improve the density. Since copper melts at 1083°C, it is expected that the Cu addition will lower the liquid formation temperature

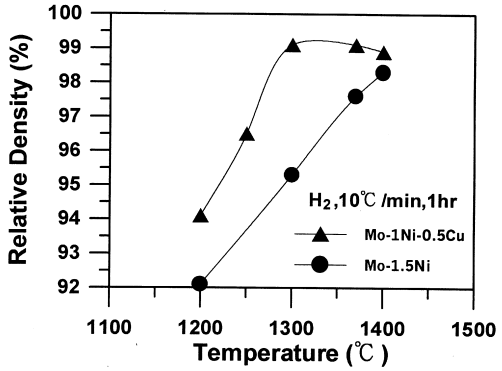

Fig. 4. The effects of sintering temperature on the density of Mo–1.5 wt.% Ni and Mo–1.0 wt.% Ni–0.5 wt.% Cu.

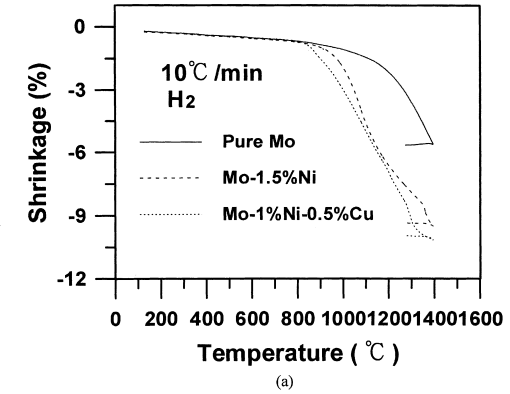

(a)

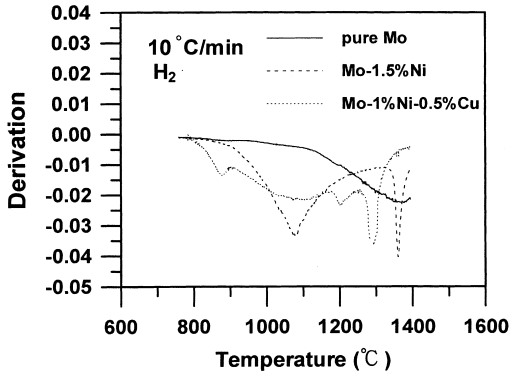

(b)

Fig. 5. (a) The dilatometer curves, and (b) their derivatives of Mo compacts with Ni and Cu additions.

of the Mo–Ni compact. This decrease of the melting point of the Mo–Ni system has been postulated, but no detailed number was reported [14]. The dilatometer curve in Fig. 5 shows that the copper did lower the liquid formation temperature from 1360°C for the Mo–1.5 wt.% Ni to 1270°C for the Mo–1.0 wt.% Ni–0.5 wt.% Cu. It is also noted that most shrinkage had occurred prior to the liquid formation. Thus, the sintering enhancement of the Mo–1.0 wt.% Ni–0.5 wt.% Cu alloy is not simply caused by the low melting point of the alloy.

Fig. 6 compares the sintered density, bending strength, and the hardness of Mo–1.5 wt.% Ni and Mo–1.0 wt.% Ni–0.5 wt.% Cu. The density of Mo–1.0 wt.% Ni–0.5 wt.%

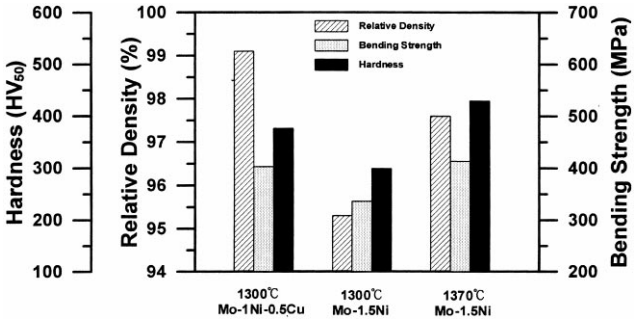

Fig. 6. The density, bending strength, and the hardness of Mo–Ni and Mo–Ni–Cu compacts sintered at 1300 and 1370°C for 1 h.

Cu compacts sintered at 1300°C was higher than those of Mo–1.5 wt.% Ni sintered at either 1300°C (activated sintering) or 1370°C (liquid phase sintering). The bending strength of Mo–1.0 wt.% Ni–0.5 wt.% Cu was 403 MPa, similar to that of liquid phase sintered Mo–1.5 wt.% Ni, but much higher than the activation-sintered Mo–1.5 wt.% Ni. The hardness of Mo–1.0 wt.% Ni–0.5 wt.% Cu compact was HV376. For Mo–1.5 wt.% Ni compacts sintered at 1370 and 1300°C, the hardness values were HV429 and HV299, respectively. The ductility was negligible in all specimens.

To understand the cause of the embrittlement, the fracture surfaces of specimens which were ruptured inside the Scanning Auger Microscope (SAM) was examined. Fig. 7a is the fractography of the Mo–1.5 wt.% Ni compact sintered at 1300°C. All fracture surfaces were of the intergranular type. In contrast, the liquid phase sintered compact, as shown in Fig. 7b, demonstrates that some cleavage surfaces were present in addition to the intergranular type of fracture surfaces. Fig. 7c of the Mo–Ni–Cu alloy also shows mixtures of intergranular and cleavage types of fracture planes.

Fig. 8a illustrates the Auger spectrum of intergranular surface (area No. 1) in the activation-sintered compact shown in Fig. 7a. Besides Mo peaks, strong Ni peaks were present. Areas No. 2 and 3 showed similar spectra. This suggests that Ni was segregated at the grain boundaries. These surfaces were then sputtered with Ar ions for different lengths of time. Results showed that no nickel was present on area No. 1 after 1 min of sputtering, indicating that the thickness of this Ni-rich layer was about 10 Å. Since this Ni-rich layer was detected on all intergranular surfaces, 10 Å was considered for only one side. Thus, the Mo–Ni layer is estimated at 20 Å thick.

In the liquid phase sintered Mo–Ni compacts, the intergranular surfaces still show the presence of Ni, as shown in Fig. 8b, similar to what was found in the activation-sintered compact. However, the sputtering experiments indicated that the thickness of this Ni-segregated layer is about 300 Å, much thicker than that in the activation-sintered compacts. The Auger spectrum of the intergranular surface of the liquid phase sintered Mo–1.0 wt.% Ni–0.5 wt.% Cu in Fig. 8c is similar to that of the Mo–1.5 wt.% Ni alloys. No copper was detected. Fig. 9 shows the Auger spectrum of the cleavage plane of Mo–Ni compact shown in Fig. 7b; in this compact, no nickel was found. The cleavage planes of Mo–Ni–Cu compact did not show any Ni or Cu peaks, either.

In addition to the Auger analyses, Fig. 10a–c shows the SEM microstructures and the X-ray mapping of the Mo–1.5 wt.% Ni compacts sintered at 1300, 1350, and 1400°C, respectively. The photographs show that the sintering was in the liquid phase at 1400°C, while at 1300 and 1350°C, the sintering was in the solid state. The X-ray mapping shows that Ni was uniformly distributed in the liquid phase. In the activation-sintered compact, nickel was located at the interstices among Mo grains. The grain size was also smaller than that in the liquid phase sintered compact.

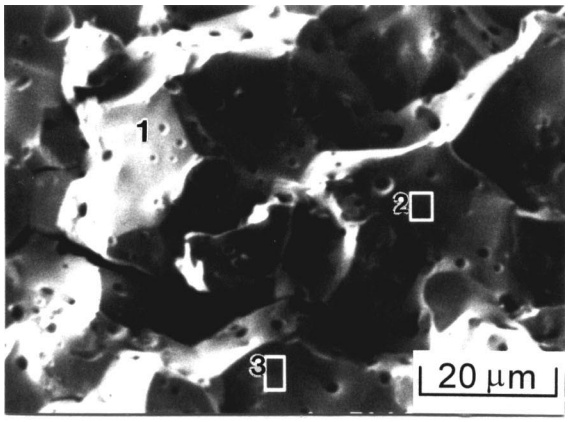

(a)

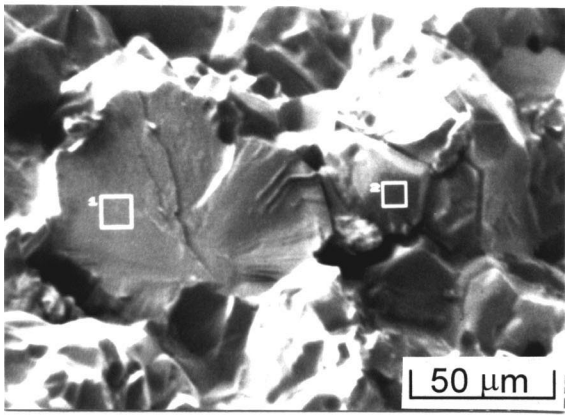

(b)

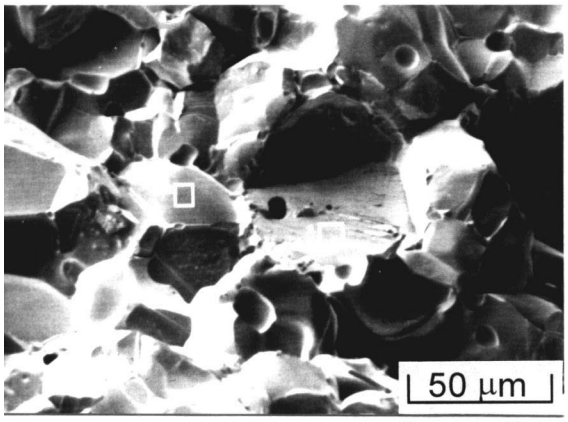

(c)

Fig. 7. (a) Intergranular fracture surfaces in the Mo–1.5 wt.% Ni compacts sintered at 1300°C; (b) mixed intergranular and cleavage fracture surfaces in the Mo–1.5 wt.% Ni compact sintered at 1370°C; and (c) mixed fracture surfaces in the Mo–1.0 wt.% Ni–0.5 wt.% Cu compact sintered at 1300°C.

Table 2 of the EPMA analysis shows that the Ni-rich clusters in the activation-sintered compact contained about 48 at.% Ni. Further tests also indicated that increasing the amount of Ni in the compact did not change the composition, only the amount of the Ni-rich areas. These results suggest that the Ni-rich clusters and possibly the thin inter-particle layers in activation-sintered Mo–Ni compact

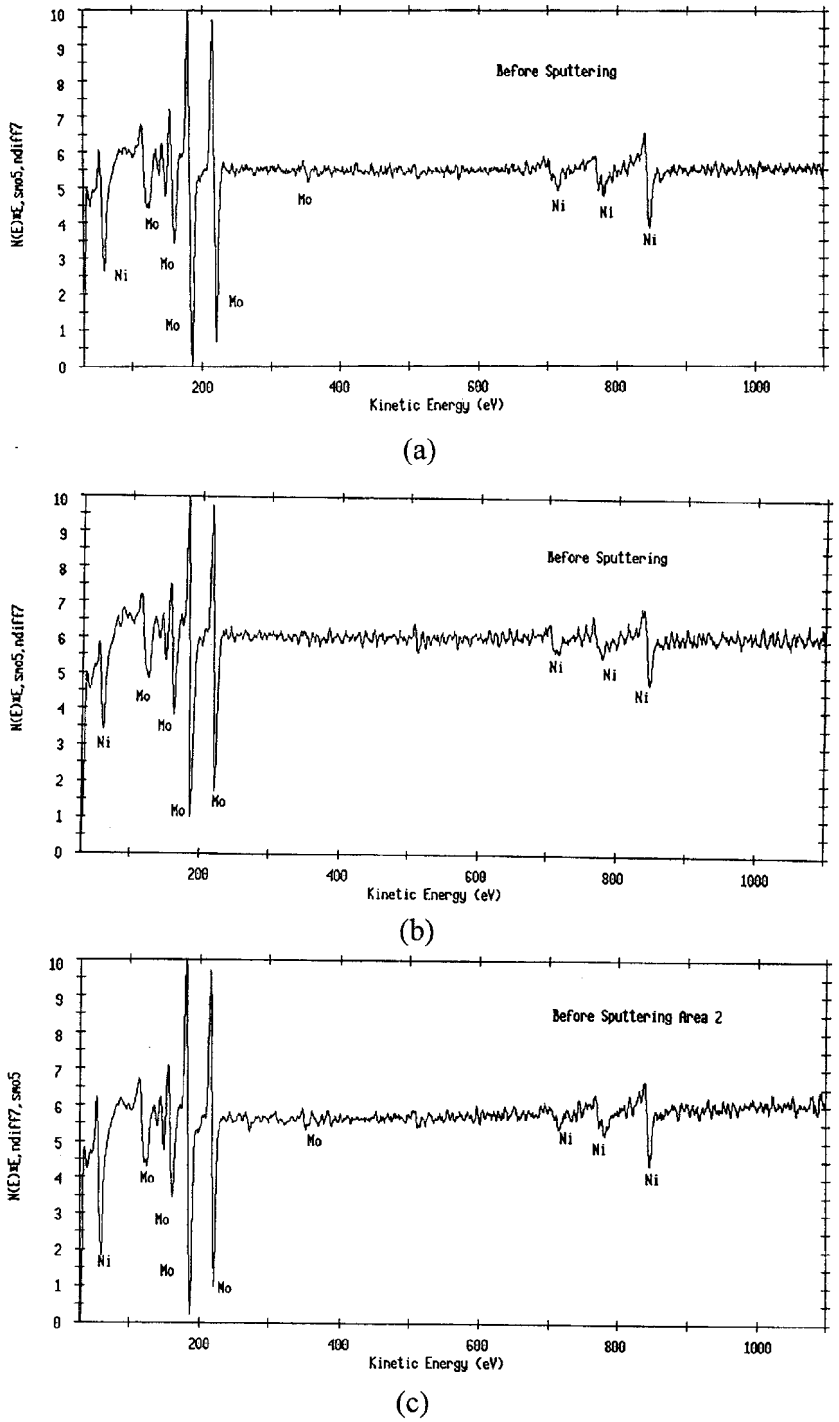

Fig. 8. The Auger spectra of the in situ fractured intergranular surfaces of the compacts shown in Fig. 7: (a) Mo–1.5 wt.% Ni, 1300°C; (b) Mo–1.5 wt.% Ni, 1370°C; (c) Mo–1.0 wt.% Ni–0.5 wt.% Cu, 1300°C.

were Mo–Ni intermetallic compounds in which the Ni content ranges from 46.0 to 48.1 at.% [15]. To examine the content of the liquid phase in the compact sintered at 1400°C, specimens were both quenched and furnace-cooled from the sintering temperature. Table 2 shows that the Ni-rich areas in quenched specimens deviated from the stoichiometry to 65.12 at.% Ni, which is reasonable as compared to the nickel compositions at the eutectic (64.2 at.%) and the peritectic (61.6 at.%) temperatures as shown in Fig. 11 [15]. The furnace cooled specimen, however, still contained about 48 at.% Ni, the same as that in activation-sintered compacts.

To further examine the structure of the liquid phase, a high Ni high Cu compact, Mo–4 wt.% Ni–2 wt.% Cu, was also sintered at 1300°C. Fig. 12 indicates that the liquid

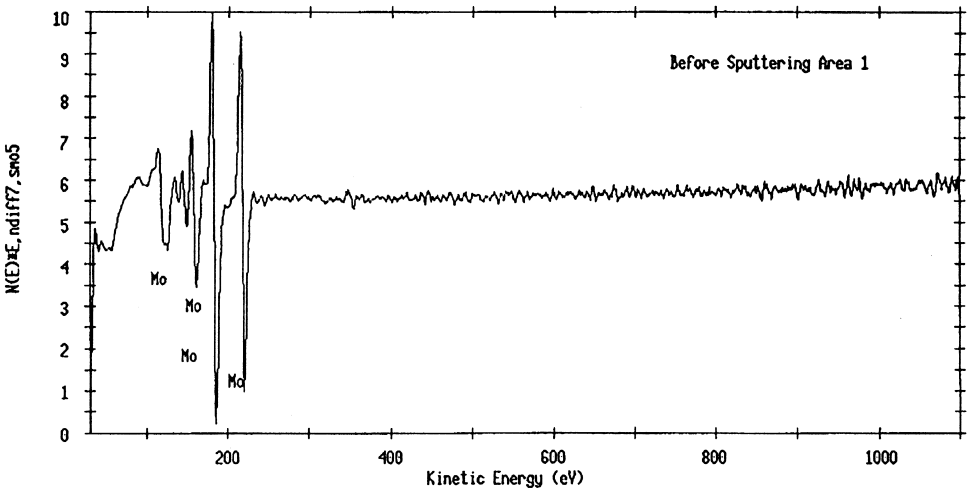

Fig. 9. The Auger spectrum of the in situ fractured cleavage surface of the Mo–1.5 wt.% Ni compact showing no nickel peaks.

separated into two phases, which differs from what is shown in Fig. 10c of the Mo–Ni compacts. The results of the EPMA analysis, as shown in Table 3, show that the composition of the light colored liquid phase in Fig. 12 consists mainly of Ni and Mo, with Cu less than 2 at.%. In comparison, the dark liquid phase was enriched with Cu and Ni. The composition of this Cu-rich area is, however, not uniform. Another test on Mo–1.0 wt.% Ni–0.5 wt.% Cu also showed the same lack of homogeneity results. Further detailed studies will be necessary to better understand the evolution of these phases.

4. Discussion

4.1. Mechanical properties

It has been postulated that, during activated sintering, nickel forms a layer and provides a short-circuit diffusion path for the molybdenum atoms [3,4,6]. Figs. 7a and 8a confirm that a Ni-rich layer was uniformly distributed on the molybdenum particle surface. This layer was only about 20 Å thick, about 10 monatomic layers. The nickel in these layers accounts for less than 1 wt.% of the nickel. Thus, most of the nickel added was still located at the original sites among molybdenum particles, as shown by the X-ray mapping in Fig. 10a. When the compact with the same nickel content was sintered in the liquid phase, the thickness of the Ni-rich layer increased to 300 Å, and the rest of the nickel was in the liquid phase. The EPMA analysis given in Table 2 suggests that the Ni-rich cluster in the compact sintered at 1300°C, the liquid phase in the compact sintered at 1400°C, and very possibly the thin Ni-rich layer between Mo particles are Mo–Ni intermetallic compounds. It is reasonable to believe that the poor ductility of the Mo–Ni compacts is attributed to this thin Ni-rich layer surrounding the Mo particles. By increasing the thickness of the Ni-rich layer, such as in the liquid phase sintered compact, or by changing the composition away from the Mo–Ni stoichiometry, such as in the specimen quenched from 1400°C, the Mo–Ni compacts still showed no ductility.

The measured Vickers hardness of the Mo–Ni compound area in the liquid phase sintered compact was HV980, similar to the HV950 reported by Schwam and Dirnfeld [16]. However, this compound is very brittle, as was noticed by the cracks around the indentation marks. Thus, to improve the ductility of the Mo–Ni compact, the intrinsic brittleness of the Ni-rich layer must be solved.

When copper was added into the Mo–Ni alloy, two distinct liquid phases formed. One consisted of 52.0 at.% Mo, 46.6 at.% Ni, and 1.4 at.% Cu, similar to the composition (52 at.% Mo, 48 at.% Ni) of the brittle Mo–Ni compound. The other liquid phase had a high copper content. However, the grain boundaries between Mo par-

Table 2
The EPMA quantitative analysis of the nickel-rich area in Mo–1.5 wt.% Ni compacts sintered at different temperatures

Temperature (°C)	Cooling condition	Mo (at.%)	Ni (at.%)
1300	Furnace cooled	51.36	48.64
1350	Furnace cooled	51.69	48.31
1400	Furnace cooled	52.29	47.71
	Quenched	34.88	65.12

Table 3
The EPMA quantitative analysis of the liquid phase in Mo–Ni–Cu compacts sintered at 1300°C

	Mo–1 wt.% Ni–0.5 wt.% Cu		Mo–4 wt.% Ni–2 wt.% Cu	
	Light colored area	Dark area	Light colored area	Dark area
Mo (at.%)	52.03	1.90∼25.06	49.89	1.81∼15.97
Ni (at.%)	46.60	23.90∼32.33	48.33	27.23∼38.71
Cu (at.%)	1.37	50.84∼65.77	1.78	56.81∼62.16

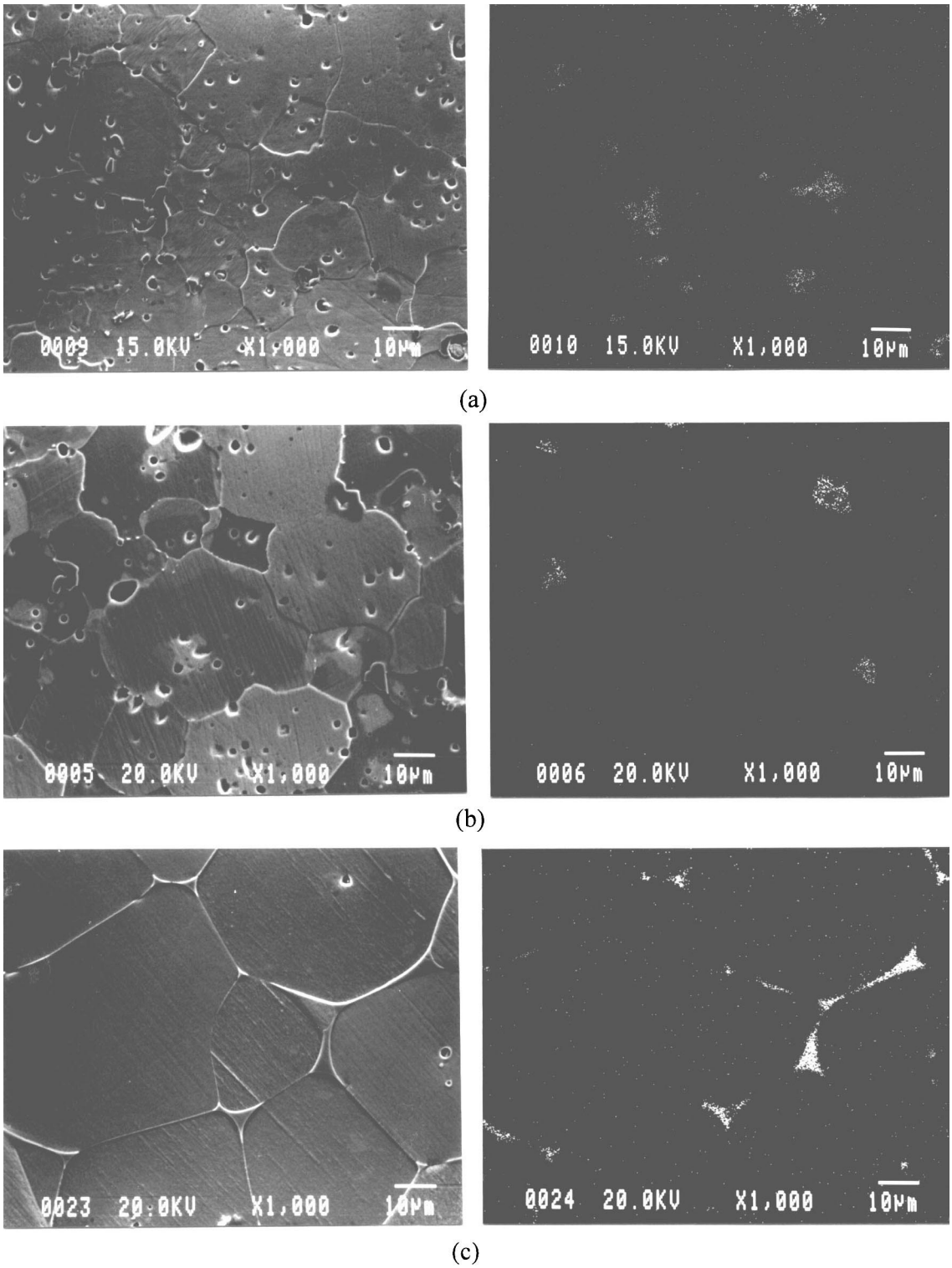

Fig. 10. The microstructure and the X-ray mapping of nickel element in Mo–1.5 wt.% Ni compacts sintered at (a) 1300°C, (b) 1350°C, and (c) 1400°C.

ticles still contained mainly the Mo–Ni layer as shown by the Auger spectrum in Fig. 8c. Thus, the ductility of the compact was still negligible. To improve the ductility of the Mo–Ni or Mo–Ni–Cu compact, the composition and/or the properties of this brittle Mo–Ni layer must be modified first. Ductility improvement studies by adjusting sintering parameters and by adding other elements to retard the formation or to alter the properties of the Mo–Ni compound should be worthwhile and are currently underway.

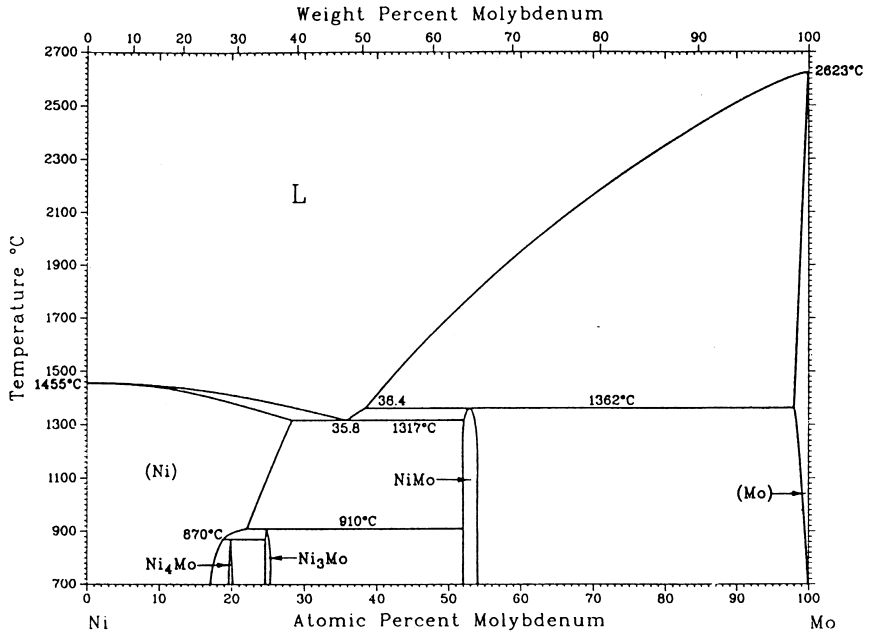

Fig. 11. Mo–Ni binary phase diagram [15].

4.2. Density

The dilatometer curves shown in Fig. 5 indicate that melting of the Mo–Ni alloy occurred at the peritectic point of 1362°C, instead of the eutectic point at 1317°C [15]. The microstructure in Fig. 10b also confirms that when the compact was sintered above the eutectic temperature at 1350°C, no liquid phase formed. This suggests that most, if not all, nickel formed a Mo–Ni compound during heating and thus no melting occurred when the eutectic temperature of 1317°C was reached. When copper was added into the Mo–Ni alloy, the copper was also dissolved in the Mo–Ni system because no melting occurred at 1083°C, as was indicated by the dilatometer curve. The melting point at about 1270°C confirms the postulation of Gupta [14] that the addition of Cu is expected to decrease the melting points of the Mo–Ni alloy.

The increase in Mo–Ni density by the addition of copper could be caused by the switch from the solid state activated sintering to the liquid phase sintering. However, the dilatometer curves in Fig. 5 show that the copper enhancement had already occurred during heating in the solid state. Since there is little intersolubility between Mo and Cu, the sintering enhancement during heating could be caused by the copper dissolution into Ni. This copper dissolution may have changed the ordering and the amount of defects in the

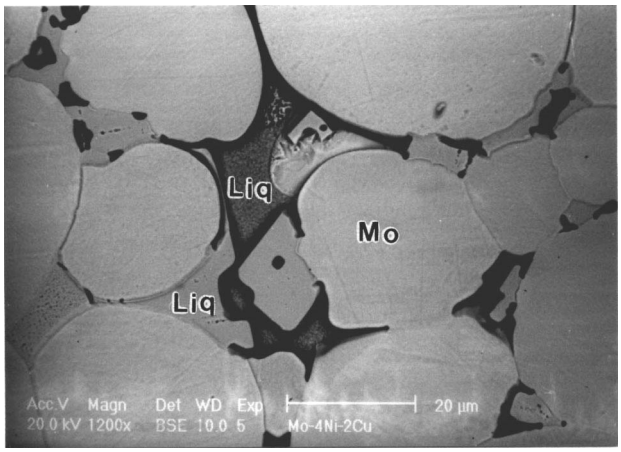

Fig. 12. The microstructure of the Mo–4.0 wt.% Ni–2.0 wt.% Cu compact sintered at 1300°C.

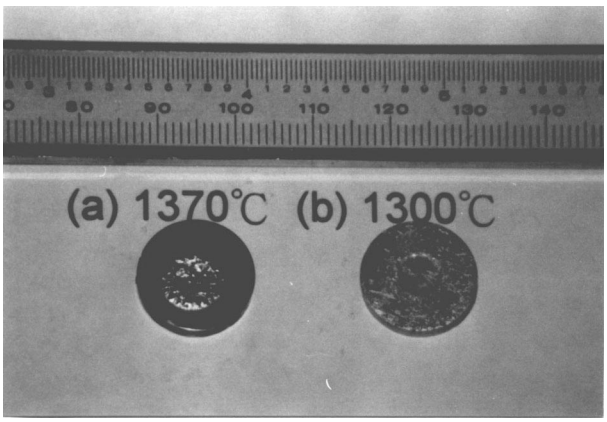

Fig. 13. Comparison of the wetting area of (a) Ni disc on Mo disc at 1370°C, and (b) Ni–33.3 wt.% Cu disc on Mo disc at 1300°C.

nickel, leading to a higher diffusion rate of molybdenum atoms.

The improved density of Mo–Ni–Cu is also caused by the enhanced wetting of the liquid phase. Fig. 13 shows the wetting condition of pure Ni and Ni–33.3 wt.% Cu discs on 15.5 mm diameter Mo discs. The Ni disc was held at 1370°C for 3 h and the Ni–33.3 wt.% Cu disc was held at 1300°C for the same amount of time. Both Ni and Ni–33.3 wt.% Cu discs melted. The Cu-containing disc wet the Mo completely, while the pure Ni did not.

5. Conclusions

With the addition of 1.5 wt.% nickel, the densities of Mo compacts increased from 82.1 to 95.5% and from 86.0 to 97.5% when sintered at 1300 and 1370°C, respectively. When 0.5 wt.% of nickel was replaced by copper, the sintered density of the Mo–1.0 wt.% Ni–0.5 wt.% Cu compact increased further to 99.1% at 1300°C. The addition of copper lowers the melting point from 1360°C, the peritectic temperature of Mo–Ni, to 1270°C. It also enhances the sintering during heating in the solid state. Better wetting was also observed and was considered a contributing factor in the improved density. The compact, though very dense, has no ductility. The brittleness of both activation and liquid phase sintered Mo compacts is very likely caused by the formation of the brittle Mo–Ni intermetallic compound at the grain boundaries.

Acknowledgements

The authors wish to thank the National Science Council of the Republic of China for their support of this work under contract number NSC89-2216-E-002-021.

References

[1] R.M. German, C.A. Labombard, Int. J. Powder Metall. Powder Technol. 18 (1982) 147.
[2] H. Hofmann, M. Grosskopf, M. Hofmann-Amtenbrink, G. Petzow, Powder Metall. 29 (1986) 201.
[3] P.E. Zovas, R.M. German, K.S. Hwang, C.J. Li, J. Met. 35 (1983) 28.
[4] J.T. Smith, J. Appl. Phys. 36 (1965) 595.
[5] J.H. Brophy, H.W. Hayden, J. Wulff, Trans. Metall. Soc. AIME 221 (1961) 1225.
[6] R.M. German, Z.A. Munir, J. Less-Common Met. 58 (1978) 61.
[7] P.E. Zovas, R.M. German, Metall. Trans. A 15 (1984) 1103.
[8] Y.V. Milman, M.M. Ristic, I.V. Gridneva, D.V. Lotsko, I. Kristanovich, V.A. Goncharuk, Poroshk. Metall. 290 (1987) 55.
[9] Metals Handbook, Vol. 7, 9th Edition, ASM, Metals Park, OH, 1984, p. 476.
[10] K.S. Churn, R.M. German, Met. Trans. A 15 (1984) 331.
[11] T. Sakamoto, J. Jpn. Soc. Powder and Powder Metall. 44 (1997) 689.
[12] K.Z. Ma, China Molybdenum Industry, Vol. 19, 1995, p. 14.
[13] T. Sakamoto, T. Honda, H. Miura, K. Okazaki, Mater. Trans. JIM 38 (1997) 326.
[14] K.P. Gupta, Phase Diagrams of Ternary Nickel Alloys, Vol. 1, Indian Institute of Metals, Calcutta, 1990, p. 179.
[15] M.F. Singleton, P. Nash, Binary Alloy Phase Diagram, Vol. 3, 2nd Edition, ASM, Metals Park, OH, 1990, p. 2635.
[16] D. Schwam, S.F. Dirnfeld, Mater. Sci. Eng. A 122 (1989) 253.